

Corrosion Behavior of Alumina/Al and SiC/Al
Metal Matrix Composites

IPEN-DOC-

5194

P.C.R. Nunes,
Comissao Nacional de Energia Nuclear,
Instituto de Pesquisas Energeticas e Nucleares,
C.P. 11049, Cidade Universitaria,
Sao Paulo 05422-970,
Brazil.

L.V. Ramanathan,
Comissao Nacional de Energia Nuclear,
Instituto de Pesquisas Energeticas e Nucleares,
C.P. 11049, Cidade Universitaria,
Sao Paulo 05422-970,
Brazil.

Abstract

Particle reinforced Al base metal matrix composites (MMC) are being considered for a range of applications. Their mechanical properties have been investigated in detail but only limited information is available about their corrosion behavior. This paper describes the influence of (a) alloy composition, (b) particle characteristics such as composition, size, volume fraction, pretreatment and (c) anodization of the composites on the aqueous corrosion behavior of Al-matrix composites prepared by the melt stirring process. The corrosion tests consisted of prolonged immersion and anodic polarization measurements. The corrosion potential, E_{corr} , and the pitting potential, E_p , of the alloys and the composites varied by upto 500 mV in deaerated solutions. Particle addition affected E_p and not E_{corr} . Immersion test data revealed significant specimen weight loss for the composites, due mainly to formation of pits or microcrevices in the matrix close to the particle/matrix interface. The pits formed in SiC composites were deeper than those in the alumina composites. This is attributable to the higher cathodic reactivity of the SiC particles. The mechanism by which pit initiation and propagation takes place is related to the presence of weak spots in the air formed film and to oxygen reduction at the particles or precipitates. Anodization improved the pitting resistance of the composites.

Key terms : Metal matrix composites, Al matrix, particle reinforcements, aqueous corrosion, pitting.

Introduction

Of the various "new" metallic materials, metal matrix composites are anticipated to have a significant niche in industries such as defence, aerospace, automotive and sports equipment. The combination of properties such as high modulus and stiffness, low

density and reduced coefficient of thermal expansion are the main attributes to ensure their place. Presently, a significant amount of data is available about the mechanical properties and correlations between processing route, microstructure and properties of MMCs. However, only limited information is available about their environmental stability. This aspect is closely associated with the presence of heterogeneities, and MMCs have a large quantity of heterogeneities in the form of the reinforcement, microcrevices, voids, porosity as well as precipitates. Although MMCs encompass a very wide range of matrix/reinforcement combinations, the aluminium alloy/SiC (or alumina) particle combination seems to be one of the most interesting for industrial applications. These composites can be produced by a variety of techniques and although the powder metallurgy route has been used quite extensively, the molten metal route is considered to be cost effective for large scale production.

A few corrosion studies on SiC/Al base alloy MMCs have focussed on the effects of reinforcement material on pitting potential, pit morphology and general corrosion susceptibility in chloride solutions (1-3). Trzaskoma et.al. observed that the pitting susceptibility of a number of common matrix alloys did not alter upon addition of SiC (1). They also found the MMCs to be less resistant to pit initiation. Paciej and Agarwala, investigating the effects of processing variables, found that a high extrusion ratio and modified solution heat treatment enhanced the corrosion resistance of alloy AA 7091/SiC composites (4). McIntyre et. al. reported that the precipitation behavior of heat treatable matrix alloys to alter the pitting susceptibility in the presence of SiC (5). It has also been shown that changes taking place at the matrix/reinforcement interface affect mechanical behavior of MMCs (6). These changes are due to a combination of one or more of the following: matrix alloy, particle surface characteristics, processing route and subsequent heat treatment. The interfacial changes are usually in the form of variations in local composition, formation of precipitates, or other reaction products, and these affect corrosion behavior. This paper describes the effects of particle composition, volume fraction, matrix alloy, particle pretreatment, and MMC surface treatment on the aqueous corrosion behavior of Al matrix composites.

Materials and Methods

Materials

Alloy AA 2014 (Al-4.5Cu-1Si-0.8Mn-0.5Mg) and Al-7.5Si-1Mg were used for preparing the MMCs. The composites preparation procedure consisted of adding preheated (and where relevant, pretreated) particles of either SiC or alumina to a vigorously stirred bath of the molten alloy. After 10 minutes agitation, the composite was poured into chilled copper molds and allowed to solidify. Particles of varying sizes were used and composites with different particle volume fraction were prepared. The particle pretreatments

consisted of (a) preoxidation of the SiC particles at 1100° C in air for 2 hours, and (b) electroless nickel plating of alumina particles from a chloride bath for 10 minutes followed by rinsing. The composite processing parameters such as melt temperature, stirrer design, stirring rate and duration, which affect reinforcement distribution were maintained at their optimized values to obtain uniform particle distribution (7). The MMC surface treatment consisted of anodization in 16 wt% sulphuric acid at 23°C and 27 mA cm (~ 18V) for 30 minutes followed by sealing in boiling water for 30 minutes. Specimens, 10x10x3mm were cut from the prepared composites for corrosion measurements.

Corrosion Measurements

The corrosion evaluation consisted of (a) long term immersion tests in 3.5% NaCl at 25° C for 28 days and (b) anodic polarization in 3.5% NaCl. Specimens of the various composites listed in Table I were prepared for the long term tests by grinding to 600 grit, degreasing and rinsing. The weighed specimens were suspended within a temperature controlled bath of NaCl. The pH was maintained constant at 7. After the test, the specimens were cleaned in 50vol% HNO₃, dried and weighed. The specimens for the electrochemical measurements were cut to size (5x5x3mm), cold mounted in epoxy resin, ground to 600 grit, rinsed and introduced into a standard corrosion cell. The specimens were allowed to equilibrate prior to measurement of the corrosion potential, E_{corr} , and initiation of anodic potentiodynamic polarization scans from -1400mV to +100mV at 10mV/s. The potential vs current curves were recorded. Measurements were carried out in both aerated and deaerated NaCl solutions. Deaeration was achieved by bubbling nitrogen through the electrolyte before and during the measurements. In tests carried out to study pit morphology, the specimens were exposed to 3.5% NaCl at 50mV above the pitting potential for 15 minutes. The specimens were rinsed thoroughly and examined in a scanning electron microscope with analytical attachments.

Results and Discussions.

Microstructural Aspects

The as cast microstructures of alloys AlSiMg and AA 2014, and their composites revealed primary dendrites, silicon particles and in the case of the composites the reinforcement particles (figure 1). The reinforcement can be observed to be well distributed. Significant improvements in particle distribution were achieved by controlling the composite processing parameters. Nevertheless, particle clustering could not be completely eliminated.

Electrochemical Measurements

The anodic polarization curves of alloy AlSiMg, AA 2014 and the composites in aerated and deaerated NaCl solutions were found to

be similar and Figure 2 shows typical curves in aerated and deaerated NaCl. The pitting potential E_p , denoted by the potential at which the current increases was read from these curves. Tables II and III list E_p and E_{corr} of the different specimens. In deaerated NaCl, E_p of the AlSiMg alloy and its composites were 300-500 mV higher than their corresponding E_{corr} . This difference in potential was observed for both alumina containing and SiC containing composites. The addition of either SiC or alumina particles to AlSiMg did not alter the corrosion potential in deaerated or aerated NaCl. These observations differ from those of Mahn and Roepstorff, who reported increase in E_{corr} with addition of and further increase in SiC to Al-SiC composites (8). In aerated NaCl, the difference between E_p and E_{corr} reduces to ~ 100 mV. This is due mainly to an increase in E_{corr} of the alloy and the composites in aerated solutions. Aeration of NaCl brings about only a slight increase in the E_p of the alloy and the composite. The addition of alumina or SiC to the alloy slightly increased the pitting potential. On the other hand, increase in particle size or quantity did not significantly alter E_{corr} and E_p .

Regarding the effects of particle treatments on electrochemical parameters, it can be observed that the composites with nickel plated alumina exhibited E_{corr} higher than that of the alloy or composites with unplated alumina. The increased E_{corr} can be attributed to the more noble nickel. Pre-oxidation of SiC particles did not affect the E_{corr} or E_p of the composites in both aerated or deaerated solutions.

Table IV lists the E_{corr} and E_p values of the as cast and anodized SiC reinforced composites of alloys AlSiMg and AA 2014 in aerated NaCl. It can be observed that both E_{corr} and E_p of alloy AA 2014 are higher than those of alloy AlSiMg. Anodization of the alloys increased both E_{corr} and E_p . The pitting potential of the anodized composite specimens were significantly higher than those of the as cast composites indicating the increased resistance of the anodized specimens to pit. Improvements in pitting resistance of anodized SiC composites were also reported elsewhere (1).

Long Term Immersion Tests

Weight loss data for the alloy and the composite specimens following 28 days immersion in 3.5 NaCl are given in Table V. It can be observed that the extent of corrosion was considerable in all cases, and provoked by pitting of the matrix. The extent of corrosion of the unreinforced alloy decreased upon addition of 5 vol% particles. Increase in SiC particle content increased

corrosion rate, whereas increase in alumina content decreased corrosion rate. This behavior may be attributed to the differences in electrical conductivity of the two types of reinforcements. Preoxidation of the SiC particles did not significantly alter long term corrosion behavior of the matrix. This may be due to loss of the SiO_2 layer on the SiC particles during specimen preparation. The extent of corrosion of composites containing Ni plated alumina was very high, due to increased galvanic effects.

Pit Morphology

Two sets of pit morphological studies were carried out. In the first, specimens held for 15 minutes at 50 mV above E_p in NaCl were examined. In the second, the specimens exposed to 3.5% NaCl for 28 days were examined. The AlSiMg alloy exposed at a fixed potential, revealed both sporadic pits and pit clusters. In the alumina containing composites, microcrevice formation was observed at the interfacial regions and in their vicinity (figure 3a,b). In many respects, the nature of the attack was similar to that observed in the alloy. The cathodic regions in the alloy and in the alumina composites were probably the precipitated second phase particles. The microcrevice formation was more widespread in regions where alumina particle clusters were present. At higher magnifications, crystallographic facetting was also observed in the alloy and in the composite. The pits formed in SiC composites were deeper than those formed in alumina composites formed under identical conditions (figure 3c). Trzaskoma et.al. reported the formation of shallow pits in SiC/6061 composites as compared to those in the unreinforced alloy (1,9). In this investigation, it has been observed that in SiC composites, the pit sizes varied considerably from 5 to $20\mu\text{m}$. Crystallographic facetting has been observed in both the alloy and in the composites contrary to observations reported elsewhere (10).

In the as cast alloy exposed for 28 days, the pits, even though few, were deeper as shown in figure 4a. The pits were crystallographic, with no evidence of facetting. The lack of facetting could be attributed to the prolonged exposure during which preferential dissolution of the edges may have taken place. In almost all the cases, in the initial stages, the interdendritic or intergranular Si was unaffected, leading eventually to it dropping out. At higher magnifications, the intergranular regions were found to be smooth and shallow (figure 4b). In the alumina composites also, preferential dissolution of the matrix led to particle dropout. In the SiC composite, smooth hemispherical pits formed around the particles (figure 4c). After 28 days exposure, more alumina particles were in place as compared to SiC particles in the respective composites. This behavior could be attributed to the higher cathodic reactivity of the SiC particles and also to the higher NaCl concentration in this investigation as compared to that used elsewhere (1).

General Discussions

In chloride ion containing solutions aluminium alloys generally pit. This has been observed, both in the unreinforced alloy as well as in the matrix of the composite. Pits usually initiate at surface heterogeneities and in the as cast alloy or the composite matrix, these heterogeneities are one or a combination of the following: (a) casting defects, due mainly to solidification shrinkage and hydrogen liberation; (b) second phase particles or other precipitates; (c) reinforcements and (d) reinforcement/matrix interaction products. In this investigation the total number of intermetallic precipitates were found to be considerably higher in the composite than in the unreinforced alloy subjected to identical treatments. Similar observations were reported by Trzaskoma (9). Consequently, candidate sites for pit initiation in the composites were significantly higher. In the unreinforced alloy, the intermetallic precipitates were the cathodic sites, whereas in the composites, depending on the composition of the reinforcement, the second phase precipitates or the interfacial reaction products were the cathodic sites for the oxygen reduction reaction.

The extent of pitting of composites reinforced with Ni plated alumina was significantly more than those reinforced with as received alumina. This behavior is attributable to the electrochemically more noble Ni envelope being efficient cathodic sites for oxygen reduction.

Mechanism

The fact that (a) in quiescent aerated chloride ion containing solutions, unreinforced and reinforced Al alloys pit spontaneously and (b) in aerated NaCl the corrosion potential of the Al alloys is more negative than in deaerated NaCl, the primary driving force in aerated media is the cathodic reduction of oxygen. In the unreinforced alloy, due to the poor conductivity of the oxide film, the oxygen reduction reaction is confined to localized areas of the surface associated with impurities or precipitates. Hence, when unreinforced alloy specimens are exposed to aerated NaCl, they reveal only a few deep pits. The introduction of ceramic reinforcements increase the density of heterogeneities, which in turn affects the electrochemical and corrosion behavior of the alloy. Since SiC is noble to the matrix in NaCl, it acts as a cathodic site. It has also been shown by surface analysis that the surface density of intermetallic precipitates is a factor of two greater for the reinforced alloy as compared to a similarly processed monolithic alloy (10). Consequently, in composites, the increased number of pits are due primarily to the increase in the number of weak spots in the oxide film covering these particles and precipitates.

Specific composite processing conditions also result in alteration of the particle/matrix interface composition and henceforth in the formation of crevices rather than pits. Similar data were reported

by Aylor and Moran for $\text{SiC}_w/6061$ (PM) composites (3).

Overall, it can be stated that the introduction of the reinforcement into the matrix alloy gives rise to three kinds of corrosion problems. The first are associated with galvanic effects. In SiC composites, the particles are more noble. In alumina composites, galvanic coupling exists to a reduced extent between the precipitated second phases and the matrix. The second are those associated with particle/matrix reaction products. These products are generally intermetallic precipitates and the oxide on the composite surface covering these precipitates are the preferred or weak spots for pit initiation. The third involve the formation of microcrevices at the interfaces and voids. Certain interfacial defects arise from incomplete cohesion between reinforcement and matrix. At these defects local chemistry necessary to retard local repassivation is easily achieved and results in formation of crevices or trenches. In this investigation, all three forms of defects induced by particle addition have been observed, either singly or jointly. Reduction in pitting of composites can be achieved by anodization of the composite or by application of reactive element impregnated coatings.

Conclusions

1. In NaCl solutions the corrosion potential, E_{corr} of the alloys and the composites increased in the presence of dissolved oxygen.
2. The pitting potential, E_p of the alloys and the composites were not affected significantly by aeration of the solution.
3. E_p of the composites were higher than those of the alloys in aerated NaCl .
4. The particle/matrix interfacial regions were the preferred sites for pitting.
5. In the presence of the reinforcement, a significant increase in the number of precipitate particles were observed.
6. The SiC particles and the precipitated phases were the sites for cathodic oxygen reduction in the SiC and alumina composites, respectively.
7. The pits were crystallographic in nature and those in SiC composites were deeper than those formed in the alumina composites.
8. Microcrevice formation was also observed, due possibly to particle/matrix decohesion.

9. Particle addition gives rise to three kinds of corrosion related problems: galvanic effects; particle/matrix reaction product induced effects; and interfacial microcrevicing.
10. Anodization of composites increases pitting resistance.

References

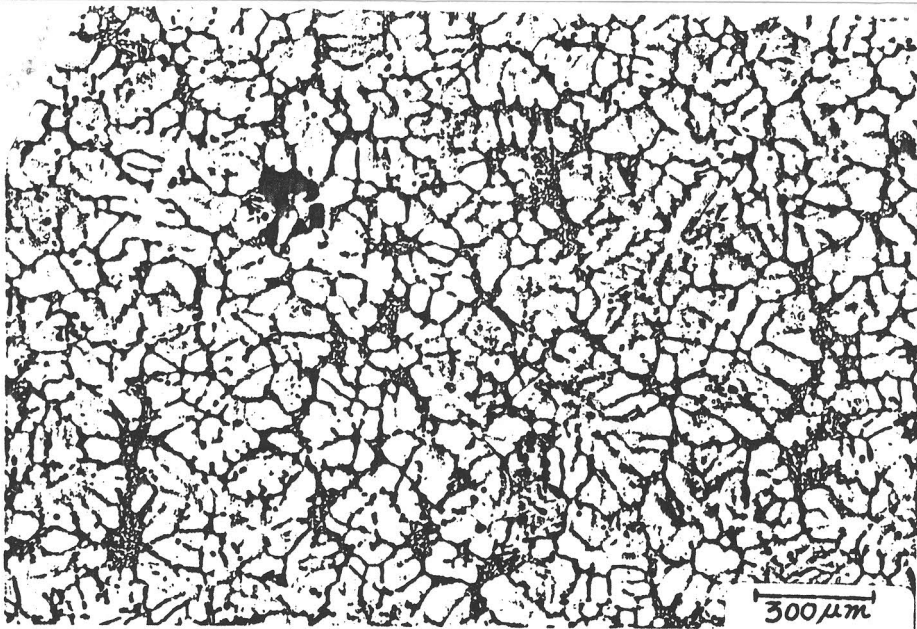
1. P.P. Trzaskoma and E. McCafferty, J. Electrochem.Soc., 130,9,(1984),p.1804.
2. M.Metzger and S.G. Fishman, Ind. Eng. Chem. Prod. Res. Dev., 22, 2,(1983),p. 296.
3. D.M. Aylor and P.J. Moran, J. Electrochem.Soc., 132,6,(1985), p.1277,
4. R.C. Paciej and V.S. Agarwala, Corrosion, 44, 10,(1988),p. 680.
5. J.F. McIntyre, R.K. Conrad and S.L. Golledge, Corrosion, 46,11, (1990),p.902.
6. D.J. Llyod, H.P. Legace and A.D. McLeod in "Controlled Interphases in Composite Materials, ICCI-III", Ed. H. Ishida, Elsevier,(1990),p. 359.
7. L.V. Ramanathan, Proc. 12th Riso Int. Symp. on "Metal Matrix Composites", Ed. N. Hansen et.al.,(1990),p. 611.
8. E. Maahn and S. Roepstorff, Proc. 12th Riso Symp on "Metal Matrix Composites", Ed. N. Hansen et. al,(1990),p. 497.
9. P.P. Trzaskoma, Corrosion, 46, 5,(1990),p. 402.
10. A. Turnbull, British Corr. J., 27, 1,(1992),p. 27.
11. L. Salvo, M. Suery, G.L. Legoux and G. l'Esperance, Mat. Sci nd Engg., A135,(1991),p.129.

Figure 1. Optical micrographs of as cast (a) AlSiMg alloy and (b) alumina composite.

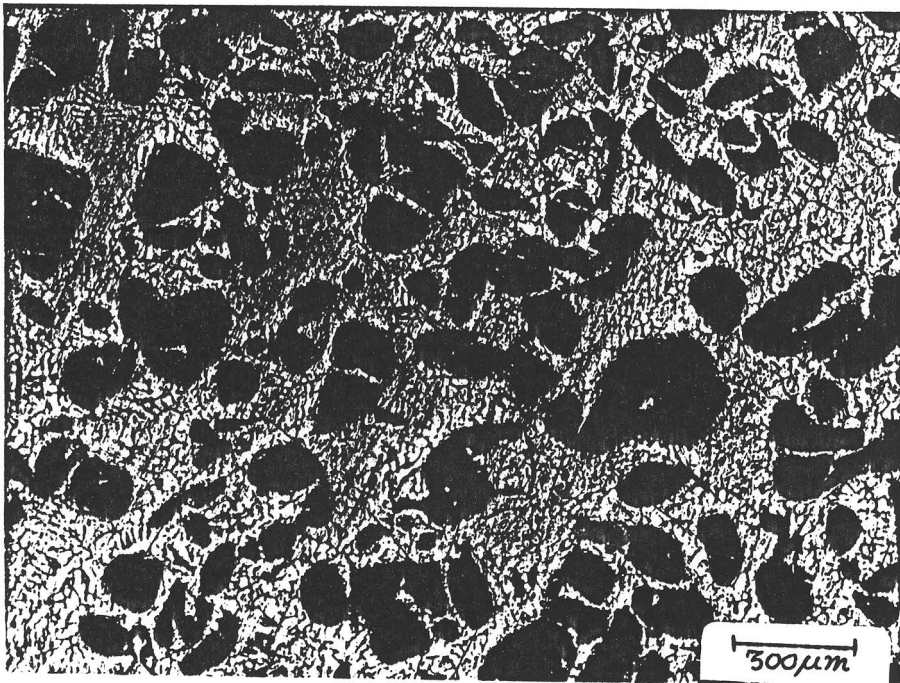
Figure 2. Anodic potentiodynamic polarization curves of alloy AlSiMg in 5% NaCl. (a) aerated (b) deaerated.

Figure 3. Scanning electron micrographs of (a),(b),alumina composite and (c) SiC composite surfaces exposed for 15 minutes at 50mV above E_p in 3.5% NaCl.

Figure 4. Scanning electron micrographs of (a) (b) AlSiMg alloy, (b) alumina composite and (c) SiC composite exposed to 3.5% NaCl for 28 days.

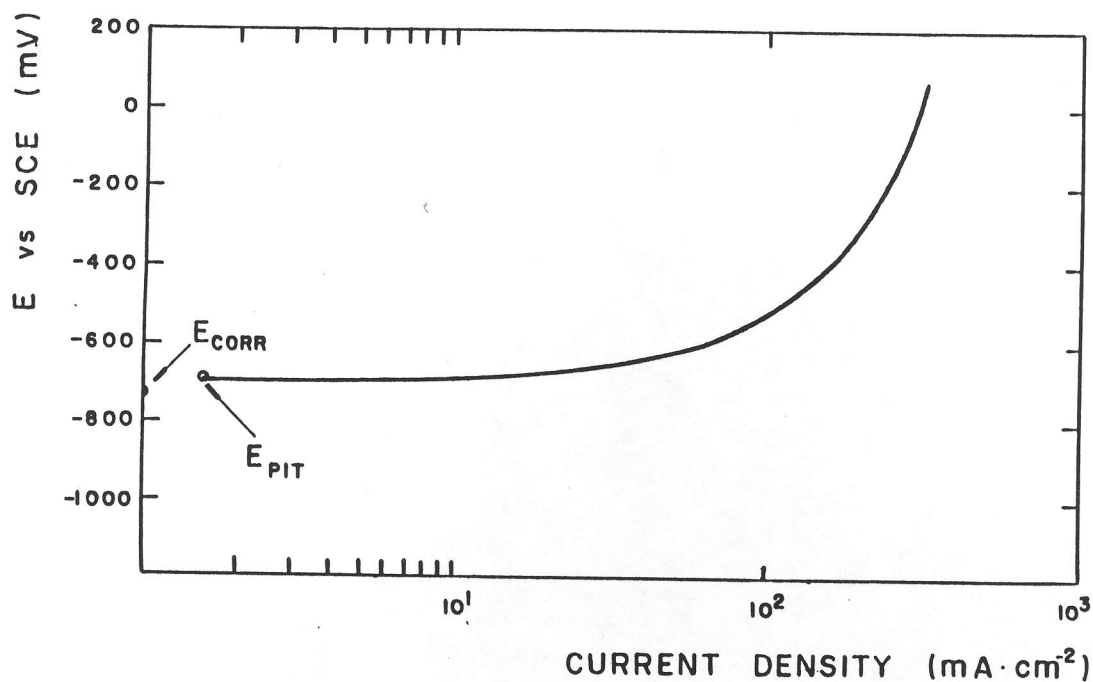


(a)



(b)

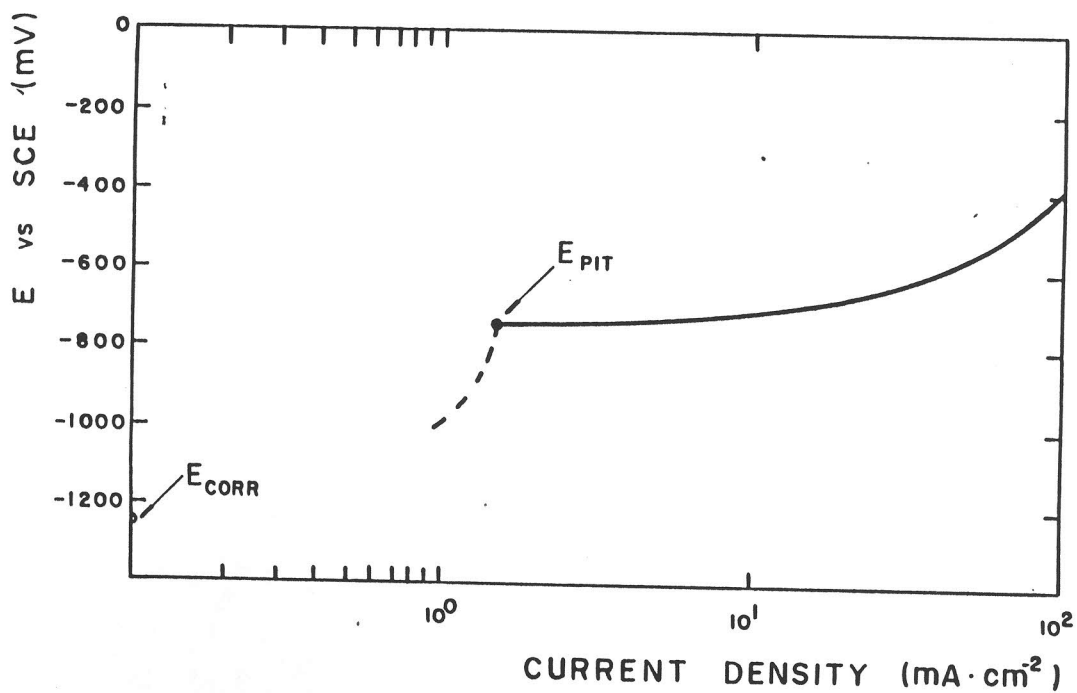
figure 1



(9)

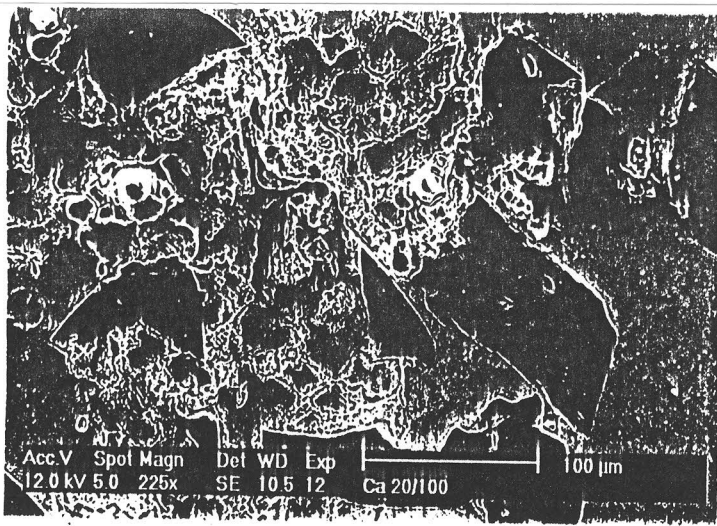
(12)

Figure 2

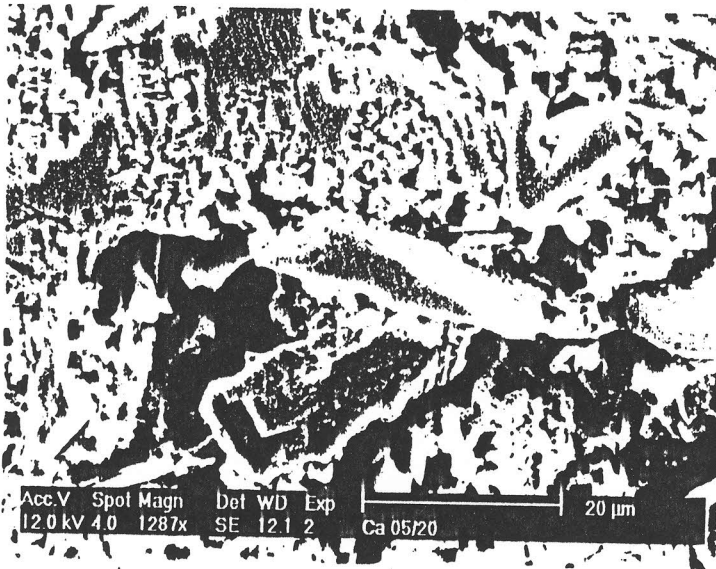


(6)

figure 2

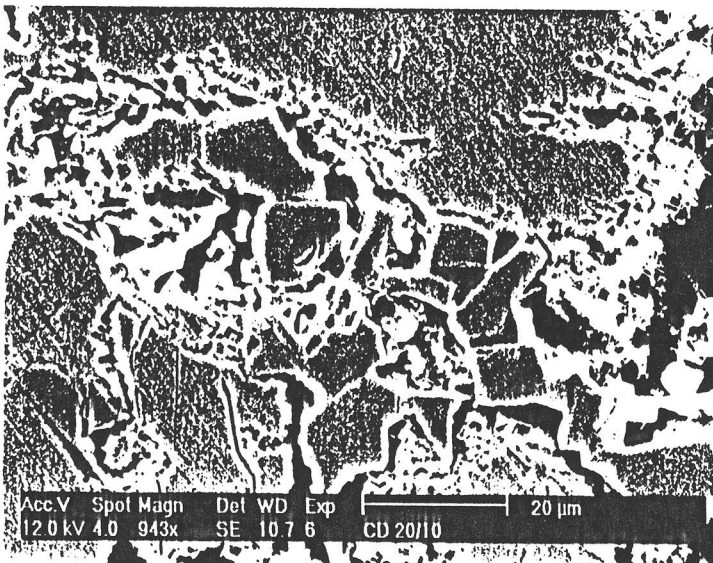


(a)

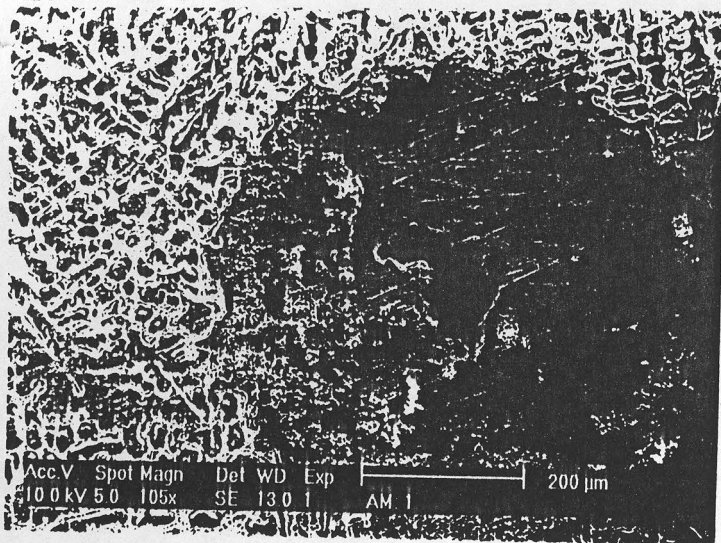


b-1

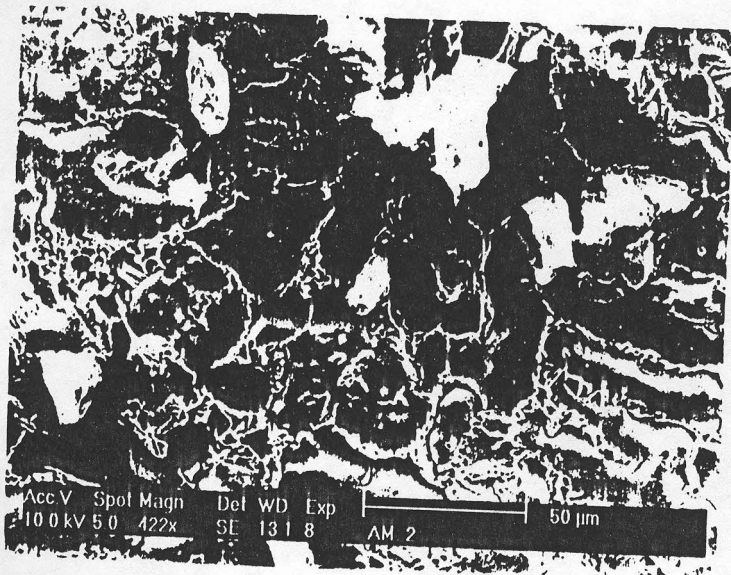
figure 3



(c)

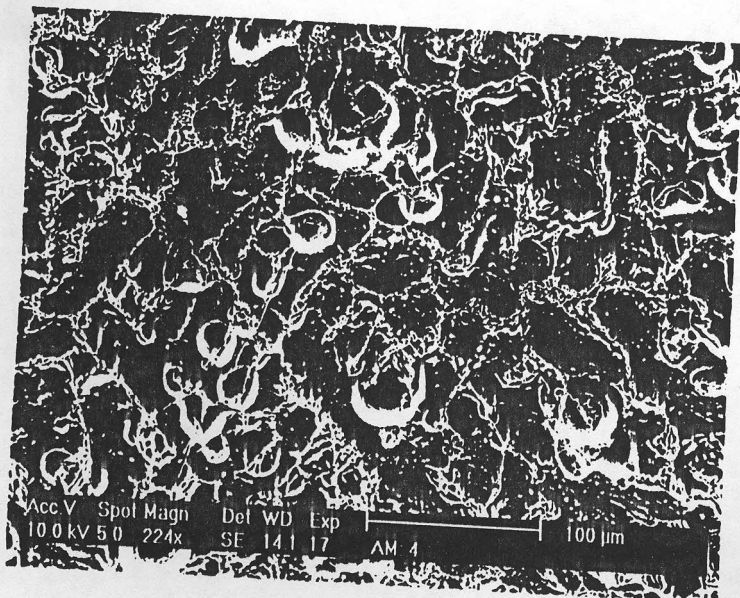


(a)



(b)

figure 4



(c)